Watershed Allied Telemetry Experimental Research

Xin Li,[1] Xiaowen Li,[2,3] Zengyuan Li,[4] Mingguo Ma,[1] Jian Wang,[1] Qing Xiao,[2] Qiang Liu,[2] Tao Che,[1] Erxue Chen,[4] Guangjian Yan,[3] Zeyong Hu,[1] Lixin Zhang,[3] Rongzhong Chu,[1] Peixi Su,[1] Qinhuo Liu,[2] Shaomin Liu,[3] Jindi Wang,[3] Zheng Niu,[2] Yan Chen,[5] Rui Jin,[1] Weizhen Wang,[1] Youhua Ran,[1] Xiaozhou Xin,[2] and Huazhong Ren[3]

[1]   The Watershed Allied Telemetry Experimental Research (WATER) is a simultaneous airborne, satellite-borne, and ground-based remote sensing experiment aiming to improve the observability, understanding, and predictability of hydrological and related ecological processes at a catchment scale. WATER consists of the cold region, forest, and arid region hydrological experiments as well as a hydrometeorology experiment and took place in the Heihe River Basin, a typical inland river basin in the northwest of China. The field campaigns have been completed, with an intensive observation period lasting from 7 March to 12 April, from 15 May to 22 July, and from 23 August to 5 September 2008: in total, 120 days. Twenty-five airborne missions were flown. Airborne sensors including microwave radiometers at L, K, and Ka bands, imaging spectrometer, thermal imager, CCD, and lidar were used. Various satellite data were collected. Ground measurements were carried out at four scales, that is, key experimental area, foci experimental area, experiment site, and elementary sampling plot, using ground-based remote sensing instruments, densified network of automatic meteorological stations, flux towers, and hydrological stations. On the basis of these measurements, the remote sensing retrieval models and algorithms of water cycle variables are to be developed or improved, and a catchment-scale land/hydrological data assimilation system is being developed. This paper reviews the background, scientific objectives, experiment design, filed campaign implementation, and current status of WATER. The analysis of the data will continue over the next 2 years, and limited revisits to the field are anticipated.

1.   Introduction

[2]   The Watershed Allied Telemetry Experimental Research (WATER) is a simultaneous airborne, satellite-borne, and ground-based remote sensing experiment taking place in the Heihe River Basin, the second largest inland river basin in the arid regions of northwest China. WATER is first of all a multiscale land surface/hydrological experiment in a cold and arid region. Hydrological processes and their roles are crucial for the socioeconomic development and for the harmonious coexistence of human beings with ecological environments. The hydrological processes are very compli-

cated, particularly in cold and arid regions, and increasingly disturbed by anthropogenic activities. However, little is known about the changes, and the hydrological, ecological and environmental impacts of these processes. Land surface experiment has proven as an effective way to promote our understanding of the terrestrial water cycle [*Avissar and Nobre*, 2002; *Goutorbe et al.*, 1994; *Sellers et al.*, 1992, 1995]. Many land surface experiments have been implemented, and arid and cold regions were paid some attention but need to be further investigated. The arid region experiments which have taken place so far include the HAPEX [*Goutorbe et al.*, 1994], HEIFE [*Hu et al.*, 1994; *Wang*, 1999], IMGRASS [*Lü et al.*, 2005], and NWC-ALIEX [*Zhang et al.*, 2005]. The most comprehensive cold region experiment carried out was the CLPX [*Cline et al.*, 1999]. All of these experiments focused on large-scale atmosphere-canopy-soil interaction with the purpose to improve GCMs and land surface models used in GCM. Other scales such as slope and mountain watershed were not considered. Therefore, in the arid and cold regions, the land surface observations, both remotely sensed and in situ, need to be significantly strengthened for a better understanding of hydrological and ecological processes at various scales.

[1]Cold and Arid Regions Environmental and Engineering Research Institute, Chinese Academy of Sciences, Lanzhou, China.
[2]Institute of Remote Sensing Applications, Chinese Academy of Sciences, Beijing, China.
[3]School of Geography and Remote Sensing Science, Beijing Normal University, Beijing, China.
[4]Institute of Forest Resource Information Techniques, Chinese Academy of Forestry, Beijing, China.
[5]School of Automation, University of Electronic Science and Technology of China, Chengdu, China.

[3] Second, WATER uses catchment as an integration entity. It should be able to provide reliable data for the development, improvement and verification of not only land surface models, but also distributed hydrological models and integrated watershed models. From the aspect of integrated watershed study, the lack of high-resolution, high-quality, and multiscale data sets has been a bottleneck [*Cheng et al.*, 2008a]. Therefore, the development of a multiscale, interdisciplinary and well-coordinated experiment to observe the watershed processes at different scales is urgently needed. In this respect, WATER will be a trial for establishing a watershed observing system [*Li and Cheng*, 2008], which serves both the emerging integrated watershed science and existing but need-to-be-improved integrated river basin management [*Surridge et al.*, 2007; *Uhlenbrook and Uhlenbrook*, 2006].

[4] Owing to its unique natural environment, the inland river basins in northwestern China can serve as an ideal laboratory for the study of hydrological processes at catchment scale in cold and arid regions. In these river basins, cold and arid regions coexist, and mountain cryosphere and the world's most dry land stand sharply in contrast. From the headwater to downstream, the landscape pattern is controlled by the quantity and distribution of the water resources. In the high-mountain area, glacier and permafrost exist. In middle-mountain area, alpine meadow and forest dominate. The middle and lower reaches are characterized by a desert-oasis-river landscape pattern, with agriculture well developed in middle stream and riparian ecosystem distributed along the river downstream. The diverse ecosystem and relatively close drainage system make the inland river basin an ideal place to carry out a watershed science study, from which fruitful results have been obtained (see the work of *Cheng et al.* [2008a] as a summary). However, there are still many gaps in our knowledge. For cold region hydrology, the uncertainties in precipitation are large, and some hydrological processes of frozen soil, snow and glacier are still unclear [*Kang et al.*, 2002]. For arid region hydrology, the scientific questions needed to be answered include: how to observe and simulate the high heterogeneity of precipitation? How the groundwater and surface water interacts in the thick vadose zone and complex irrigation system [*Wheater et al.*, 2008]? How to detect the natural and anthropogenic factors that influence the hydrological process [*Wang et al.*, 2003]? The answers to these questions depend on more thorough measurements using new earth observing technologies. Establishing a watershed observing system will potentially lead to a revolutionary change in watershed science and management and eventually to a more sustainable development of river basins.

[5] The initialization of WATER was based on the above background. Under the auspices of the Chinese Academy of Sciences (CAS), it was started as a CAS West Action Plan Project [*Huang et al.*, 2007], and later was jointly supported by the State Key Basic Research Project "Theory and method for a synthetic retrieval of terrestrial ecological variables from both active and passive remote sensing approaches" under the auspices of the Ministry of Science and Technology of China (MOST). After a few years planning, WATER was launched formally in July 2007 and is undergoing at full speed. Most of the intensive field campaigns in the plan have been accomplished.

[6] WATER is composed of three hydrological experiments, one crosscutting experiment, and an integrated study: (1) cold region hydrology experiment, (2) forest hydrology experiment, (3) arid region hydrology experiment, (4) hydrometeorology experiment, and (5) development of the WATER information system and a catchment-scale land/hydrological data assimilation system. This paper will introduce the background, scientific objectives, experiment design and configuration, field campaigns implementation, and current status of WATER.

2. Overview of WATER

2.1. Objectives

[7] The following key scientific questions will be explored in WATER: (1) To what extent can the hydrological and ecological variables derived from remote sensing be used to improve our understanding of cold region, arid region and forest hydrologies? (2) How can one develop more appropriate scaling approaches so that multisource and multiscale remote sensing data and in situ measurements can be used synthetically in hydrological, ecological, and integrated river basin models? (3) How can one assimilate the remote sensing and in situ measurements into the catchment-scale hydrological and ecological models in order to improve the simulation capacity and predictability of river basin dynamics?

[8] To address these questions, the overall objective of WATER was defined as follows: to improve the observability, understanding, and predictability of hydrological and related ecological processes at catchmental scale, accumulate basic data for the development of watershed science, and promote the applicability of quantitative remote sensing in watershed science studies.

[9] The immediate goals of WATER are as follows: (1) to observe the major components of water cycle in cold region, forest, and arid region hydrology experimental areas by carrying out a simultaneous airborne, satellite-borne, and ground-based remote sensing experiment in the Heihe River Basin; (2) to develop scaling methods using airborne high-resolution remote sensing data and intensive in situ observations, and improve the remote sensing retrieval models and algorithms for water cycle variables and corresponding ecological and other land surface variables/parameters; (3) to use all the available data in the validation, improvement and development of catchment-scale hydrological and ecological models, as well as decision support tools for water resource management; (4) to develop a catchment-scale land/hydrological data assimilation system, which is capable of merging multisource and multiscale remote sensing data to generate high-resolution and spatiotemporal consistent data sets in order to improve the predictability of water cycle and its response to environmental changes; and (5) to establish a public experiment field and develop open and free, multiscale, and integrated data sets for the development of watershed science.

2.2. Experimental Area

[10] The experiment was carried out in the Heihe River Basin, China's second largest inland river basin. It is located between $97°24'\sim102°10'$ E and $37°41'\sim42°42'$ N and covers an area of approximately 130,000 km². Landscapes
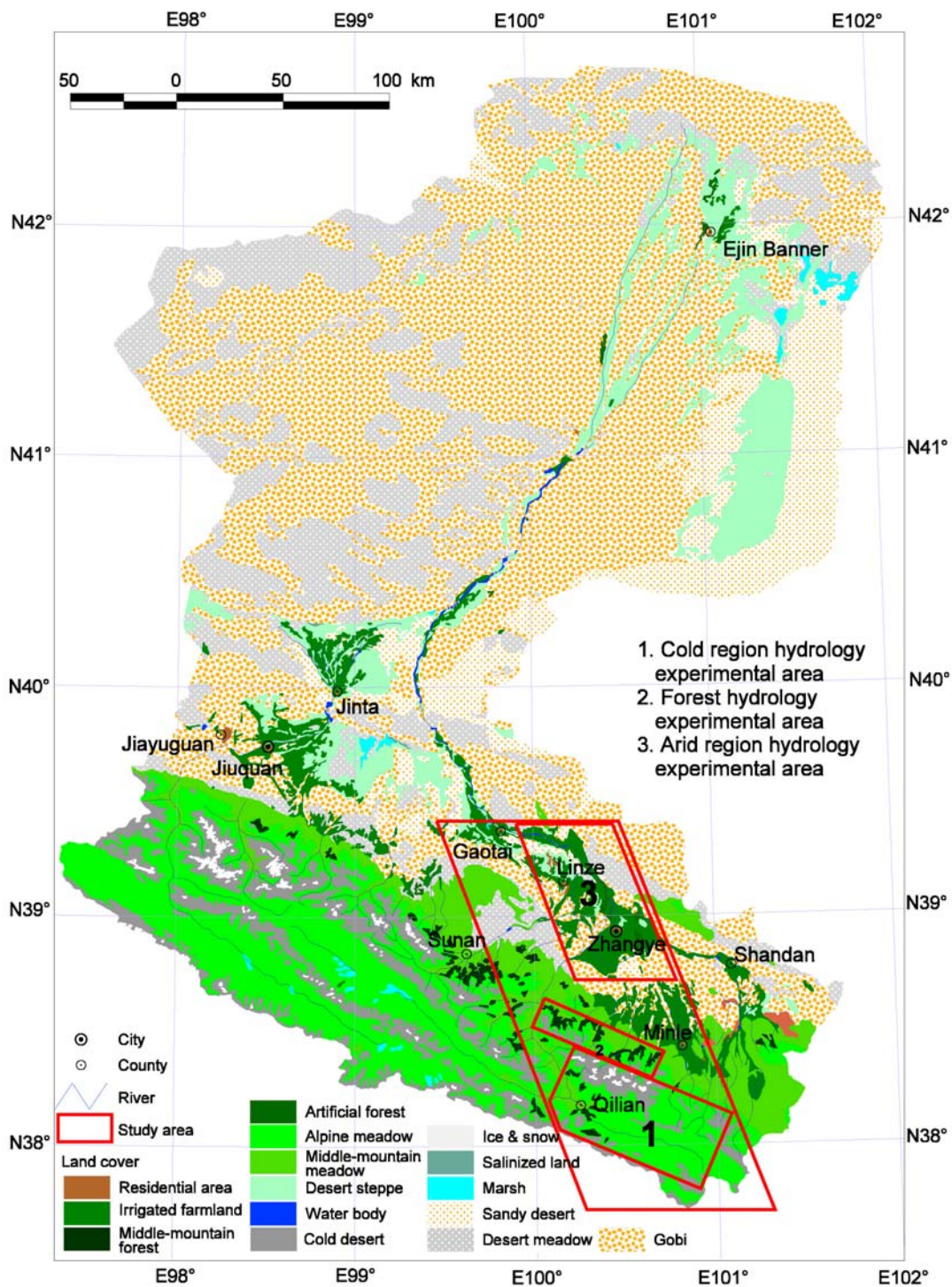
Figure 1. Heihe River Basin and the location of three key experimental areas (the background is the landscape map of the Heihe River Basin).

are diverse; from the upper to down stream, glacier, frozen soil, alpine meadow, forest, irrigated crops, riparian ecosystem, desert, and gobi are distributed (Figure 1).

[11] The Heihe River Basin was equipped with good research facilities and rich data sets [*Cheng et al.*, 2008a; *Li and Cheng*, 2008]. Much research on inland river basins used it as a case study. More background of the Heihe River

Basin can be found in the work of *Li et al.* [2001], *Wang and Cheng* [1999], and others.

[12] WATER was implemented at four scales, with different observing strategies used in different scales.

[13] 1. The first scale is the whole river basin, on which the satellite remote sensing is employed.

[14] 2. The second scale is the key experimental area (KEA), which represents three key hydrological processes

in an inland river basin, that is, cold region, forest, and arid region hydrologies. Correspondingly, three key experimental areas were identified. They are the cold region hydrology experimental area in the mountain cryosphere of the upper reaches, forest hydrology experimental area in the forest-steppe zone of the upper reaches, and arid region hydrology experimental area in the oasis-desert zone of the middle reaches (Figure 1).

[15] 3. The third scale is the foci experimental area (FEA), which is embedded within the KEA. The FEA was setup with a high priority for simultaneous airborne, satellite-borne and ground-based measurements. In addition, the hydrological, ecological and atmospheric variables that are not retrievable from remote sensing are also measured intensively in FEAs. They were identified by considering the representativeness of the hydrological processes in inland river basin as well as the existing observation facilities, transportation accessibility, logistic availability and other practical issues.

[16] 4. The fourth scale is the experiment site (ES), in which automatic meteorological stations (AMS), flux towers or other observation facilities were setup. It is the elementary unit for simultaneous ground-based observation.

[17] The cold region hydrology experimental area is located in the Babao River Basin, which is a subcatchment in the upper reaches of the Heihe River Basin. The area is 2452 km^2, and the elevation is from 3000 m to about 5000 m. Permafrost and glacier are distributed in this area, and snow prevails in winter.

[18] The forest hydrology experimental area is located on the south slopes of the Qilian Mountains. There are several watersheds with areas from tens of square kilometers to more than 100 km^2. Forests are distributed at elevations between 2800 and 3500 m.

[19] The arid region hydrology experimental area is located in the middle reaches of the Heihe River Basin. The terrain is very flat with elevations ranging from 1500 to 2000 m. The annual precipitation is very low, less than 200 mm. The artificial oasis, desert, gobi, and transitional zones between oasis and desert are dominant landscapes. The FEAs will be introduced in section 3.

2.3. Variables and Parameters to Be Observed

[20] The variables and parameters to be measured were identified from a viewpoint of integrated watershed model development, with reference to existing and frequently used land surface models (*Dai et al.* [2003] and *Sellers et al.* [1996], among others), distributed hydrological models [*Arnold and Fohrer*, 2005; *Liang et al.*, 1994; *Wigmosta et al.*, 1994], and dynamic vegetation models (*Sitch et al.* [2003], among others). They were organized into five categories, that is, hydrological and ecological variables, atmospheric forcing variables, vegetation parameters, soil parameters and aerodynamic parameters. More information can be found in the detailed experiment design [*Li et al.*, 2007, 2008]. The observation strategy is that for hydrological variables that can be retrieved or estimated from remote sensing conventionally, such as evapotranspiration (ET), snow water equivalent, snow cover extent and soil moisture, efforts would be made to improve the estimation accuracy using multisource remote sensing synthetically. For those that are not conventionally associated with remote sensing,

such as interception and stemflow, we will try to get related parameter, for example, canopy structure, from a new observing technique such as light detection and ranging (lidar), in order to link them with hydrological model. The hydrological variables that are still irretrievable from remote sensing will be measured on the ground.

2.4. Strategy for Sampling and Ground Truth Collection

[21] A three-level stratified sampling strategy was designed with reference to the sampling methods developed by other investigators [*Justice et al.*, 2000; *Liang et al.*, 2002; *Tian et al.*, 2002].

[22] 1. The first level is the FEA. In each FEA, at least one AMS or flux tower was installed, and ground-based remote sensing and other instruments were employed in the intensive field campaigns to obtain time-continuous data. The high temporal resolution observations were used not only for validation but also for developing temporal scaling methods.

[23] 2. The second level is the ES. In each FEA, several ESs were identified according to the observation aims and representativeness. The landscape and terrain within an ES should be as homogeneous as possible. There were three kinds of ES: small ES, large ES and striped ES. The small ES was in addition divided into $3 \times 3 \sim 12 \times 12$ subsites, with each one spanning a 30×30 m^2 plot. This corresponds to the pixel size of high-resolution remote sensing, such as Landsat TM and Envisat ASAR. Meanwhile, a few plots 5×5 m^2 in size were embedded in small ES, to correspond with the very high resolution airborne remote sensing. The large ES covered a 2×2 km^2 area and contained small ESs (Figure 2). It was designed to validate the medium resolution of satellite remote sensing such as MODIS. The striped ES was designed to correspond with the nonimaging airborne microwave radiometer. Several sampling strips, each of $1 \sim 2.5$ km in length and the width equaling to the resolution of microwave radiometer, were set up at right angles to the flight routes. The samples were collected every $50 \sim 100$ m along the strip.

[24] 3. The third level is the elementary sampling plot (ESP), where the samples were collected using the pixel size as an elementary unit. For different observation items, the sampling strategies were different. A random sampling method was used for relatively homogeneous ESP. A "carpet sampling" method [*Zhang*, 1996], which means very dense spatial sampling, was employed for parameters with larger spatial heterogeneity. Since the spatial resolution of the VNIR (visible and near infrared) and thermal infrared airborne remote sensing was about $1 \sim 5$ m after processing, imaging instruments such as thermal imager and Ground Penetrating Radar (GPR) were preferred.

[25] The spatial aggregation approach of in situ measurements was based on the heterogeneity and spatial structure of ESP. For very homogeneous land surfaces, the mean value of the sample measurements could be used to validate the pixel observation [*Liang et al.*, 2002]; for land surfaces with strong spatial structure, for example, desert vegetation, the fractions of vegetation and bare soil should be taken into account by upscaling [*Hufkens et al.*, 2008]; for heterogeneous land surface but without an apparent spatial structure, geostatistics was used to transfer point measure-
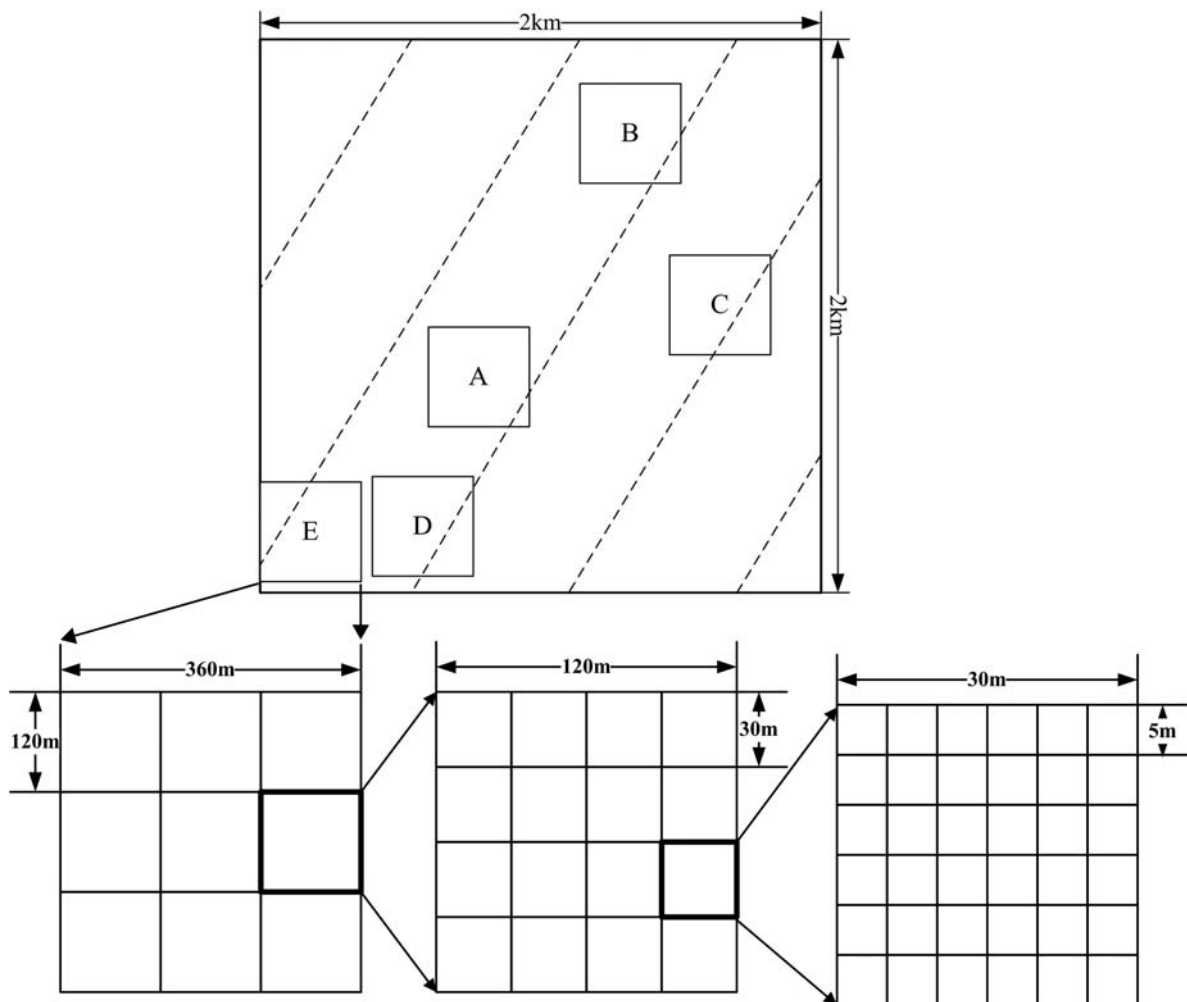
Figure 2. General scheme of the sampling strategy used in WATER.

ments into pixel value [*Goovaerts*, 1997]. It should be noted that the airborne remote sensing has a higher resolution. It is able to bridge the gap between ground observation and satellite remote sensing and therefore play very important role in WATER. Usually, the airborne remote sensing was first validated by ground measurements, and then it was used as an intermediate scale and was upscaled to less fine resolution of satellite remote sensing [*Zhang*, 1996].

[26] Temporal scaling is also of critical importance. In WATER, the temporal sampling scheme was designed as follows. For the variables or parameters that change quickly with time, such as the ET, land surface temperature (LST), and canopy temperature, the observation was carried out near the overpass of airplane. In addition, since it was not possible to carry out all the ground measurement simultaneously, owing to limited manpower, temporal scaling method must be developed on the basis of time-continuous observation from automatic instruments. For the variables or parameters that are relatively stable within hours, such as soil moisture, the measurement was carried out a few hours before or after the overpass. For the variables or parameters that are stable for several days, such as vegetation coverage, leaf area index (LAI), biomass, tree height, and roughness,

the measurement was carried out within a few days before or after the corresponding airborne mission.

2.5. Duration

[27] The life term of WATER was determined by the time needed for data collection and analysis. An annual cycle is the minimum interval required to observe the water cycle, especially those related with soil freeze/thaw; in addition, long-term monitoring is also needed for many hydrological and ecological variables. In total, four periods were determined as necessary for the implementation of WATER.

[28] 1. The first period is the experiment planning period. The idea of WATER was initialized in 2004. Then, the experiment implementation plan was circulated among many domestic and international scientists for review. WATER was formally launched in July 2007. After that, from 1 July to 31 October 2007 was the period for completion of the detailed design of the experiment, choice of airborne sensors and aircraft, establishment of the ground observation network, calibration of various instruments, ordering of remote sensing data, and collection of existing data in the Heihe River Basin.

[29] 2. The second period is the preobservation period (POP), which was carried out in the summer (July ∼ October)
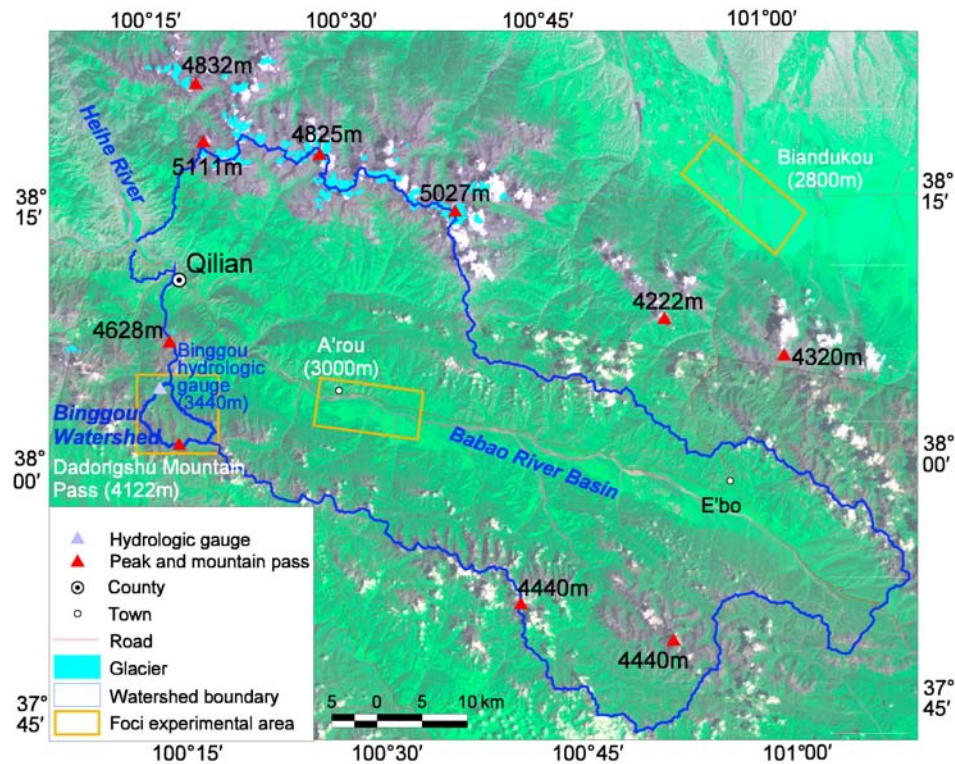
Figure 3. Cold region hydrology experimental area (the background is a mosaic of a Landsat thematic mapper (TM) image).

of 2007 in the forest and arid region experimental areas and in winter (October ∼ December) in the cold region experimental area. The most important tasks of POP were to rehearse the simultaneous experiment, verify the measurement schemes, test the instruments, and train the observers. On the basis of these, the experiment design was improved.

[30] 3. The third period is the intensive observation period (IOP). The airborne missions and intensive filed campaigns were carried out in winter (March ∼ April) 2008 in the cold region experimental area and in summer (May ∼ August) 2008 in the forest and arid region experimental areas. The automatic measurements of meteorological, hydrological and ecological processes were planned to be carried out using AMS and flux towers all year.

[31] 4. The fourth period is the persistent observation period, which would last from July 2008 to December 2009 or even longer if resources are available. Two years of continuous data collection was planned on the basis of the established ground hydrometeorological network. Limited revisits to the field and simultaneous experiments with satellite remote sensing are anticipated.

[32] Data processing and analysis, publication of results, and development of the WATER information system (WIS) are carried out through the implementation period of WATER, with more concentrated efforts after the IOP.

3. Ground Data Collection

[33] The POP was carried out from early August to mid-December 2007. The IOP was carried out from 7 March to 12 April for the cold region, 15 May to 22 July for the forest

and arid region, 23 August to 5 September for the forest hydrology experiments, in total, 120 days. During the field campaigns, numerous ground data were collected, with most of them obtained simultaneously with airborne missions (section 4) and satellite overpasses (section 5).

3.1. Cold Region Hydrology Experiment
3.1.1. Foci Experiment Areas
[34] The cold region hydrology experiment was carried out in three FEAs (Figure 3), with the key aim to observe the physical properties of snow and frozen soil.

[35] 1. The Binggou watershed (BG) is a high-mountain drainage system with an area of 30.48 km^2. The mean depth of the seasonal snowpack is about 0.5 m, with a maximum of 0.8–1.0 m. The lower limit of permafrost is about 3400 m. The aim of the measurements in BG was snow.

[36] 2. A'rou (AR) is located in the middle reaches of the Babao River Basin and is a relatively flat area with a mean elevation of about 3000 m. The seasonally frozen soil is widely distributed. The main aim of the measurements was seasonally frozen soil. Airborne remote sensing of soil freeze/thaw status was carried out.

[37] 3. Biandukou (BDK) is a flat area near Minle County, with a mean elevation of 2800 m. The algorithm to detect soil freeze/thaw status using passive microwave remote sensing was validated here. The soil moisture was another aim of the measurements.

3.1.2. Snow
[38] The depth, density, grain size, wetness, temperature, and dielectric properties of snow were simultaneously measured using a snow fork, which is a radiowave sensor, and other instruments within 9 ESs in BG during the IOP of
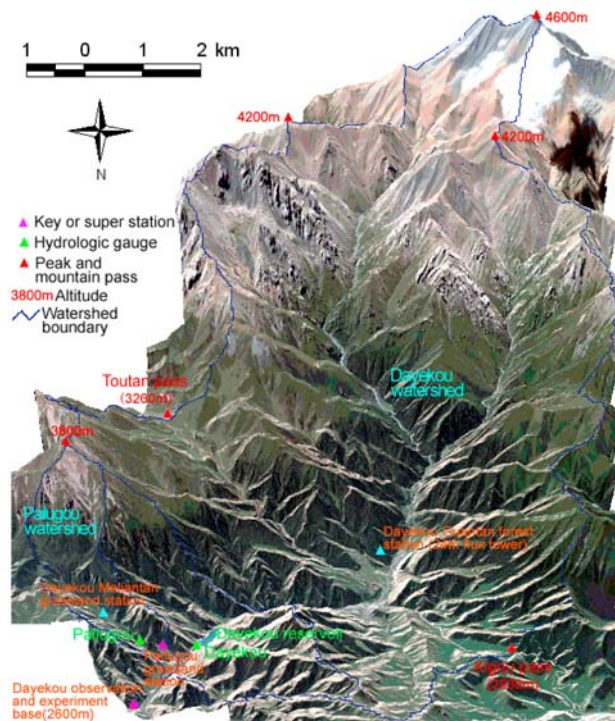
Figure 4. Forest hydrology experimental area (the background is a mosaic of a Quickbird image overlain on a high-resolution digital elevation model, DEM).

the cold region hydrology experiment. In total, 672 ESPs were used during eight ground observations. The regular observation of snowfall, evaporation, sublimation, and snowmelt started with the POP, and were made at least twice a day. The spectral reflectance and albedo of snow were measured using an analytical spectral device (ASD) and albedometer, respectively. In addition, the microwave properties of snow were observed using the ground-based Ka-band (37 GHz), K-band (18.7 GHz), X-band (10.8 GHz), and C-band (5.4 GHz) radiometers as well as a S-band (2.65 GHz) scatterometer during the overpass of airborne missions for snow.

3.1.3. Soil Freeze/Thaw Status and Soil Moisture

[39] Numerous ground truths were collected at 3 ESs in AR and 5 ESs in BDK to verify the algorithm to detect soil freeze/thaw status and retrieve soil moisture using microwave remote sensing. The liquid soil water content and soil permittivity were measured using frequency domain portable soil moisture probes (ThetaProbe soil moisture sensor and POGO portable soil sensor). Their applicability and accuracy were calibrated in the laboratory. The total water content was obtained using the gravimetric sampling method, then the ice content was calculated as the difference between total and liquid water contents. The LST and the near surface soil temperature at $0{\sim}5$ cm were measured using handheld infrared thermometer and digital thermometers, respectively. Other parameters used in the microwave remote sensing model of frozen soil, such as the surface roughness (surface height standard deviation and correlation length), vegetation water content and vegetation height were also measured in all ESPs.

[40] The microwave properties of freeze/thaw cycle were observed using a truck-mounted microwave radiometer, which has frequency modules of 18.7 and 36.5 GHz, and the S-band scatterometer in BDK and AR during the overpass of airborne missions for frozen soil. In addition, two continuous observations were carried out using the ground-based Ka-, K-, X-, C-, and S-band (3.0 GHz) radiometers in 19–25 October 2007 and 6–8 April 2008 in AR for the purpose of validating a microwave radiative transfer model for frozen soil.

[41] The GPR is potentially capable of monitoring the unfrozen water content in the active layer and to detect the frost or thaw penetration from the reflector depth. During the IOP, GPR was used in AR and BDK in selected days when airborne microwave radiometer was flown or satellite-borne SAR overpassed. Preliminary result showed that it is a promising way to capture the variation of soil moisture at pixel scale, which can provide a ground truth for microwave remote sensing of soil moisture.

3.2. Forest Hydrology Experiment
3.2.1. Foci Experiment Areas

[42] In the forest hydrology experimental area, two watersheds, Dayekou and Pailugou, were chosen as the FEAs (Figure 4).

[43] 1. Dayekou watershed (DYK) is a drainage system in the upper reaches of the Heihe River Basin, with an area of about 69 km^2. The forests are widely distributed and dominated by *Picea crassifolia*.

[44] 2. Pailugou watershed (PLG) covers an area of 2.95 km^2, with a wide range of elevations between 2600 and 3800 m. The mean annual air temperature is 0.7°C and the mean annual precipitation is about 435.5 mm. Good measuring facilities such as permanent sampling plots for forest monitoring were available in the watershed.

[45] The aims of the measurements in the two FEAs were ET, interception, stemflow, fall-through, and biogeophysical and structure parameters of forest. Three airborne remote sensing instruments including the imaging spectrometer, thermal imager, and lidar were chosen to observe the forest hydrology (section 4).

3.2.2. Structure and Biogeophysical Parameters

[46] The structure and biogeophysical parameters of forest play very important role in improving the forest hydrology modeling. Therefore, the measurements of forest type, forest density, LAI of forest canopy, forest coverage fraction, above ground biomass of forest, forest volume density, mean forest stand height, single tree height, tree crown shape and size were carried out intensively on the ground, with most of them concurrent with airborne missions of lidar and CCD, or satellite overpasses of lidar, SAR, and hyperspectral instruments. The IOPs for forest hydrology experiment took place from 1 to 13 June, in the first phase, and from 23 August to 5 September, in the second phase. The following measurement activities were carried out.

[47] A 100 × 100 m^2 supersite was established around the Dayekou Guantan forest station, where airborne lidar and CCD were flown intensively to obtain very high resolution data. The supersite was divided into a 4 × 4 subplot with a size of 25 × 25 m^2. The locations of these subplots and each tree were surveyed using total station instruments. One ground lidar system was placed at the
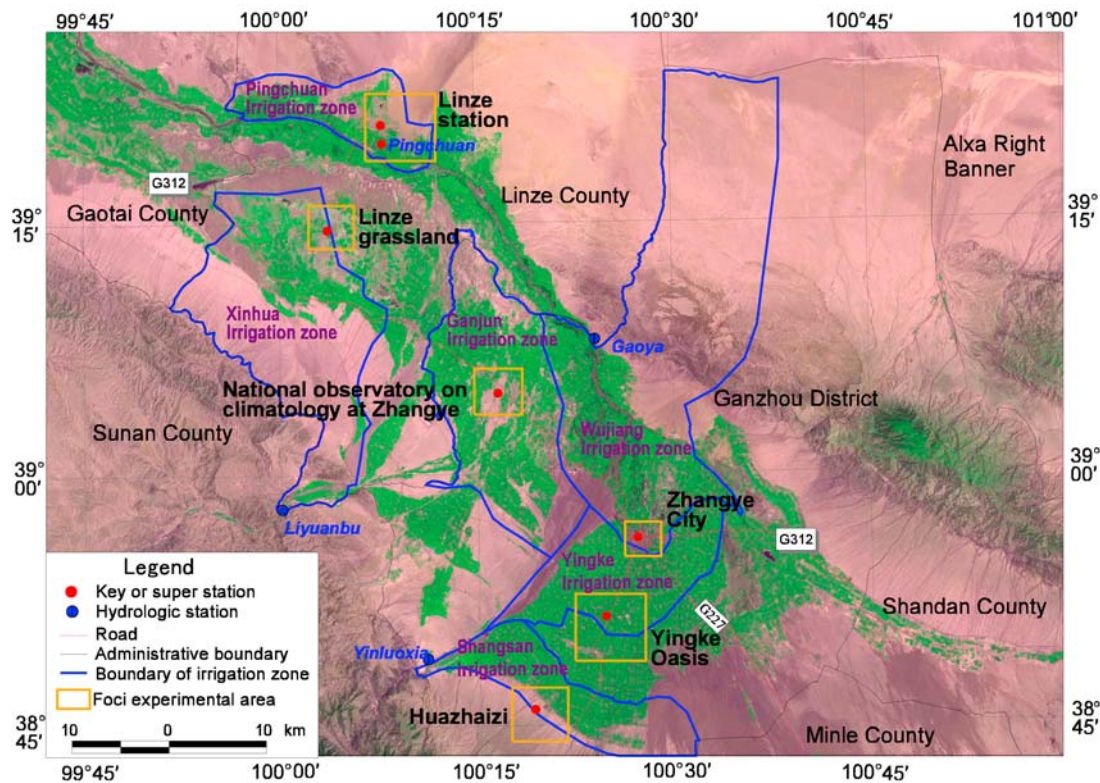
Figure 5. Arid region hydrology experimental area (the background is a mosaic of a Landsat TM image).

center of each plot to perform a 3-D scanning of the trees around it, from which the 3-D structure of the forest scene can be constructed. The diameter at breast height, crown size, full height, and tree height below main branches of each tree were measured within one subplot. The moisture of small branches and leaves of selected trees with different ages were measured using dry weighting method. The spectral reflectance of several typical land cover types and different parts of tree were measured using ASD. The bidirectional reflectance distribution function (BRDF) measurement of a small tree was also carried out. The LAI and forest canopy coverage were measured using different instruments including TRACK, LAI-2000, and HemiView. All of the above observations will be used to provide a near-true virtual forest stand scene for the development and validation of lidar and SAR signal simulation models, and forest structure parameter inversion algorithms.

[48] In addition, one forest sampling line of 20 m width and 1 km length was set up near the supersite, and 16 permanent ESPs were already distributed in DYK. During the IOP, the structure and biogeophysical parameters of forest were measured at 19 ESPs (size of 20×20 m^2) every 50 m along the sampling line, and LAI was measured at the permanent ESPs as a supplement to the annual conventional observations.

3.2.3. Hydrological Variables

[49] Intensive ground measurements of forest hydrological processes were carried out from 1 June to 30 September. Various field instrumentations were designed and installed to quantify the forest interception in the Guantan forest station and PLG. The precipitation was measured using self-

recording rain gauges and manual rain gauges. The rainfall interception for *Picea crassifolia* was measured by the trough gauges. The stemflow was measured by a stemflow collector, which is a longitudinal cutting plastic that wrapped up and adhered the bottom of the tree trunk. The water was collected in plastic bottles which were emptied in the end of every rainfall process. The rainfall holding process of the bryophyte and litter layer was also measured using interception gauges. The ET of the vegetation layers under forest was measured using microlysimeters. These observation instrumentations were installed according to different canopy gap fractions.

3.3. Arid Region Hydrology Experiment
3.3.1. Foci Experiment Areas

[50] In the arid region hydrology experimental area, six FEAs were identified, which are distributed along the middle reaches of the Heihe River from south to north (Figure 5).

[51] 1. Huazhaizi (HZZ) is located on desert steppe to the south of Zhangye oasis. The aims of the measurements were ET, soil moisture as well as biogeophysical and biogeochemical parameters of desert vegetation.

[52] 2. Yingke oasis (YK), located to the south of Zhangye city, is a typical irrigated farmland. The primary crops are maize and wheat. The aims of the measurements were ET, biogeophysical and structure parameters of crop, interaction between groundwater and surface water, and irrigation.

[53] 3. For Zhangye city (ZY), the aims of the measurements were land use and optical properties of atmosphere.
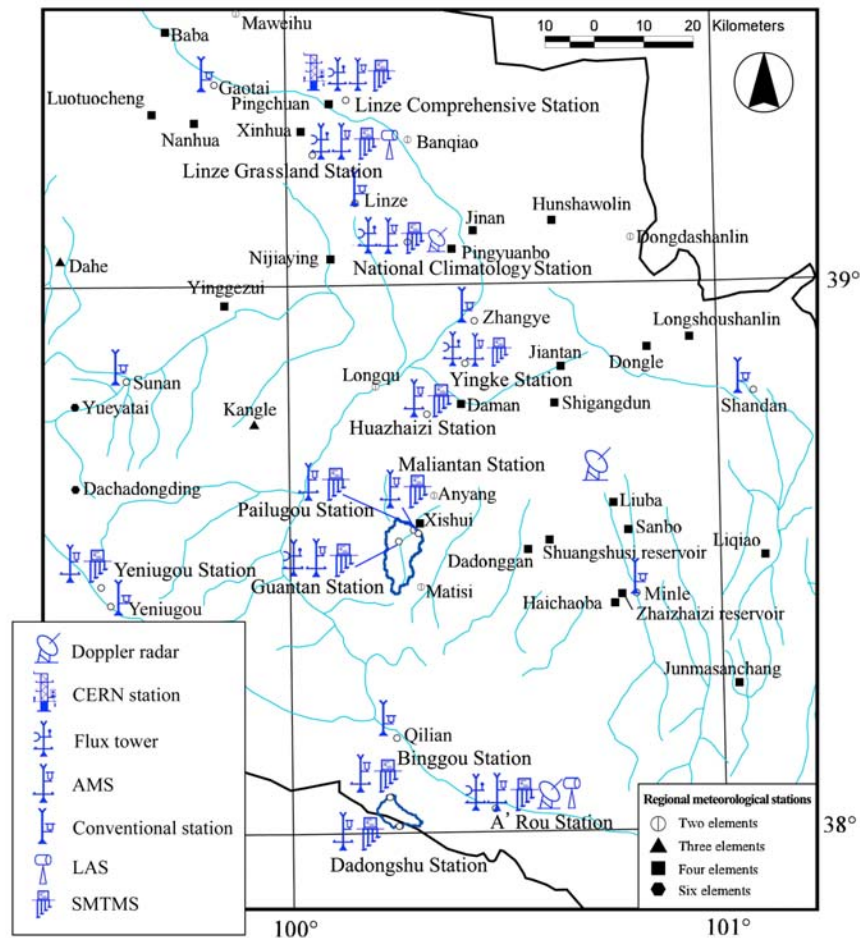
Figure 6. Network of the automatic meteorological stations and flux towers in WATER. For regional meteorological stations, two elements indicate air temperature and precipitation, three elements indicate wind direction plus two elements, four elements indicate wind speed plus three elements, and six elements indicate air pressure and global radiation plus four elements. CERN, Chinese Ecosystem Research Network; LAS, large aperture scintillometer; SMTMS, Soil Moisture and Temperature Measurement System.

[54] 4. For the National Observatory on Climatology at Zhangye (ZYNOC), landscape in the vicinity is gobi desert. In this area, the energy balance was to be measured on the basis of the existing facilities in the observatory.

[55] 5. In Linze grassland (LZG) the land cover types are diverse, with wetland, grassland, salinized meadow, and farmland distributed in vicinity. The ET, soil moisture, LST, canopy temperature, and biogeophysical parameters were to be measured at various scales.

[56] 6. Linze station (LZS) is located in the vicinity of Linze Inland River Basin Comprehensive Research Station, which is a Chinese Ecosystem Research Network (CERN) station. LZS is in the transitional zone between oasis and desert. Simultaneous observations of ecohydrology were carried out here, complemented by operational monitoring of CERN. The most important aims of the measurements were ET and dewfall.

[57] Simultaneous ground measurements for arid region hydrology were carried out in 6 FEAs, 16 ESs and more than 300 ESPs during the IOP. The main observations include ET, soil moisture, dewfall, groundwater, LST,

emissivity, spectral reflectance, albedo, and various biogeophysical, biogeochemical and structure parameters.

3.3.2. Hydrological Variables

[58] ET, as the most important hydrological variable in arid region, was measured continuously by six eddy covariance (EC) flux towers at site scale and two large aperture scintillometer (LAS) flux systems in AR and LZG at a larger scale of 1 to a few kilometers. In addition, it was measured using microlysimeters installed in DYK, YK, LZG, and LZS during the IOP.

[59] The ground measurements of soil moisture were carried out in LZG, LZS, and BDK. Numerous ground truths were collected in different landscapes, such as salinized soil, reed field, barley field, and alfalfa field. The method was similar to that used in AR, except that in some ESs in LZG, where the salt content was very high, so the gravimetric sampling method was also used to measure the soil moisture when the time domain reflectometer (TDR) was not applicable. Meanwhile, the vegetation water content and the roughness were also obtained. In addition, 16 soil moisture profile probes were installed at a reed field in

Table 1. Key Stations and Superstations in WATER

Name	Experiment	Station Type	Location	Observation Items	Landscape
A'rou freeze/thaw observation station	Cold region hydrology	Superstation	100°27′E, 38°03′N, 3033 m	Atmosphere: wind speed, air temperature and humidity (2 and 10 m), wind direction, air pressure, precipitation, and four components of radiation.[a] soil: temperature, moisture, water potential profile (10, 20, 40, 80, 120, and 160 cm), and heat flux (5 and 15 cm). EC, LAS.	Alpine meadow
Binggou cold region hydrometeorological station	Cold region hydrology	Key station	100°13′E, 38°04′N, 3407 m	Atmosphere: wind speed, air temperature and humidity (2 and 10 m), wind direction, air pressure, precipitation, and four components of radiation. soil: temperature and moisture profile (5, 10, 20, 40, 80, and 120 cm) and heat flux (5 and 15 cm).	Alpine marshy meadow
Dadongshu Mountain Pass snow observation station	Cold region hydrology	Key station	100°14′E, 38°01′N, 4101 m	Atmosphere: wind speed, air temperature and humidity (2 and 10 m), wind direction, air pressure, precipitation, snow depth, and four components of radiation. soil: temperature and moisture profile (5, 10, 20, 40, 80, and 120 cm) and heat flux (5 and 15cm).	Cold desert
Yeniugou cold region hydrological station	Cold region hydrology	Key station	99°33′E, 38°28′N, 3320 m	Atmosphere: air temperature and humidity (1.5 and 2.5 m), wind speed and direction, air pressure, precipitation, and global and net radiation. soil: temperature and moisture profile (20, 40, 60, 80, 120, and 160 cm) and heat flux (5cm). CO_2 (3.5 m).	Alpine meadow
Dayekou Guantan forest station	Forest hydrology	Superstation	100°15′E, 38°32′N, 2835 m	Atmosphere: wind speed, air temperature and humidity (2, 10, and 24 m), four components of radiation (1.68 and 19.75 m), wind direction, air pressure, precipitation, snow depth, and PAR. soil: temperature and moisture profile (5, 10, 20, 40, 80, and 120 cm), frost depth, and heat flux (5 and 15 cm). EC, sap flow (3), fall-through, stemflow.	Forest
Dayekou Maliantan grassland station	Forest hydrology	Key station	100°18′E, 38°33′N, 2817 m	Atmosphere: wind speed, air temperature and humidity (2 and 10 m), wind direction, air pressure, precipitation, and four components of radiation. soil: temperature and moisture profile (5, 10, 20, 40, 80, and 120 cm) and heat flux (5 and 15 cm).	Grassland (*Iris lacteal* dominates)
Pailugou grassland station	Forest hydrology	Key station	100°17′E, 38°34′N, 2731 m	Atmosphere: air temperature and humidity (1.5 and 3 m), wind speed (2.2 and 3.7 m), wind direction, air pressure, precipitation, and global and net radiation. soil: temperature (20, 40, 60, 80, 120, and 160 cm), moisture (10, 20, 40, 60, 120, and 160 cm), and heat flux (5 cm × 3). CO_2 (2.8 and 3.5 m), sap flow (4)	Grassland at the margin of a forest
Huazhaizi desert station	Arid region hydrology	Key station	100°19′E, 38°46′N, 1726 m	Atmosphere: wind speed, air temperature and humidity (2 and 10 m), wind direction, air pressure, precipitation, four components of radiation, and LST. soil: temperature and moisture profile (5, 10, 20, 40, 80, and 160 cm), and heat flux (5 and 15 cm).	Desert steppe
Yingke oasis station	Arid region hydrology	Superstation	100°25′E, 38°51′N, 1519 m	Atmosphere: wind speed, air temperature and humidity (3 and 10 m), wind direction, air pressure precipitation, four components of radiation, and LST. soil: temperature and moisture profile (10, 20, 40, 80, 120, and 160 cm), and heat flux (5 and 15 cm). EC.	Cropland (maize)
National Observatory on Climatology at Zhangye	Arid region hydrology	Superstation	100°17′E, 39°05′N, 1456 m	Atmosphere: wind speed, air temperature and humidity (2, 4, 10, 20, and 30 m), wind direction, air pressure, precipitation, PAR, four components of radiation, and LST. soil: temperature (5, 10, 15, 20, and 40 cm), moisture (10, 20, 50, 100, and 180 cm), and heat flux (three layers). EC.	Gobi desert
Linze grassland station	Arid region hydrology	Superstation	100°04′E, 39°15′N, 1394 m	Atmosphere: wind speed, air temperature and humidity (3 and 10 m), wind direction, air pressure, precipitation, four components of radiation, and LST. soil: temperature (5, 10, 20, and 40 cm), moisture (10 cm), and heat flux (5 cm). EC and LAS.	Wetland with saline-alkali soil
Linze Inland River Basin Comprehensive Research Station[b]	Arid region hydrology	Superstation	100°08′E, 39°21′N, 1382 m	Atmosphere: air temperature and humidity (1.5 and 3 m), wind speed (2.2 and 3.7 m), wind direction, air pressure, precipitation, and global and net radiation. CO_2 (2.8 and 3.5 m). soil: temperature (20, 40, 60, 80, 120, and 160 cm), moisture (10, 20, 40, 60, 120, and 160 cm), and heat flux (5 cm × 3). EC.	Cropland

[a]Four components of radiation indicate the total solar radiation, reflective shortwave radiation, land surface longwave radiation, and atmospheric longwave radiation.
[b]For Linze Inland River Basin Comprehensive Research Station, the EC tower is located at Wulidun (100°08′E, 39°20′N, 1378 m).
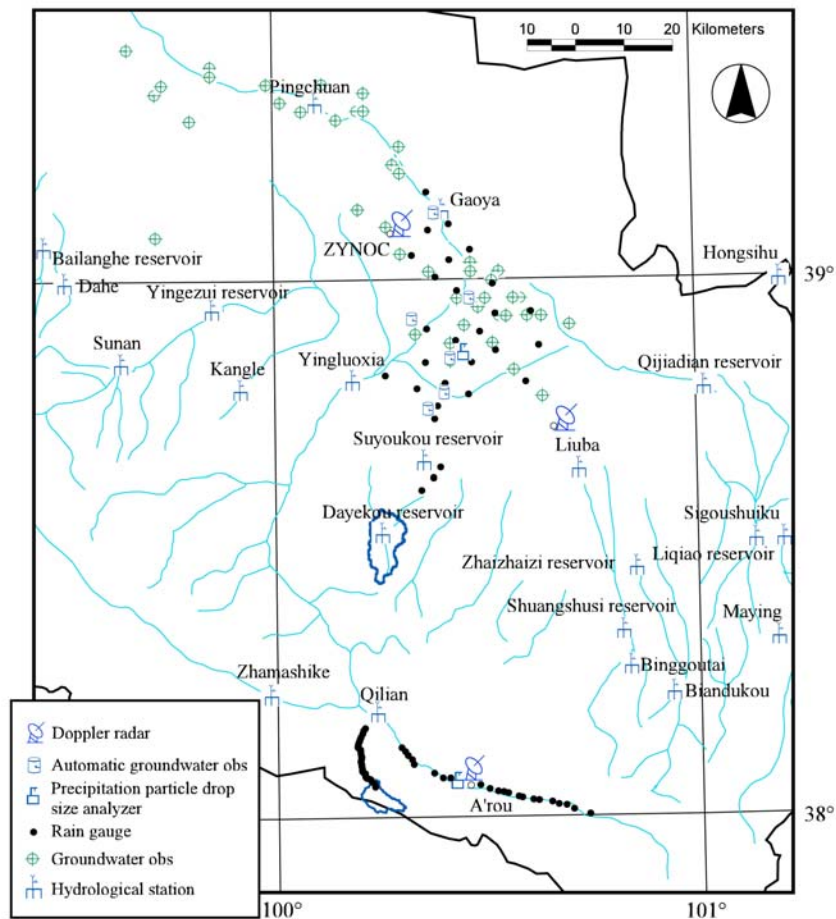
Figure 7. Precipitation and other hydrological observations in WATER.

LZG to measure the soil moisture content at 10, 20, 30, 40, 60 and 100 cm on a daily basis for the purpose of understanding the spatiotemporal variation of soil moisture and investigate the spatial and temporal scaling.

[60] The dew deposition was measured within a sand dune situated in the desert-oasis ecotone, LZS using micro-lysimeters. The daily amounts of dew were about 0.1 mm per night and they changed with a large range depending on the slope, aspect and position of the sand dunes.

3.3.3. Biogeophysical and Biogeochemical Parameters

[61] The LAI was measured nondestructively using LAI-2000 and directly using LI-3100 and LI-3000C. The latter was considered to have a higher accuracy and therefore can be used as the truth. The TRAC was used especially in the artificial forests. The leaf angle distributions (LAD) were measured using rulers and LI-3000C at the same time by establishing a relationship between leaf geometry and area.

[62] The vegetation fractional coverage was measured using the general digital camera or the special digital camera with a fisheye lens. The photos were analyzed by the WinSCANOPY or CAN_EYE vegetation canopy analysis system.

[63] The SunScan canopy analysis system was used to measure the fraction of photosynthetically active radiation (FPAR). The FPAR at different heights of the plants was measured. In addition, the FPARs of typical vegetations were measured at a half-an-hour interval from morning to evening to capture their diurnal variations.

[64] Photosynthesis and transpiration rate of leaves were measured using a portable photosynthesis system LI-6400. Leaves at different heights in the canopy were observed in order to calculate the effective photosynthesis and transpiration of the whole canopy associated with the leaf area of different leaves. The chlorophyll content of leaves was measured using a handheld SPAD-502 at the same time and same location as the LI-6400 measurements. The component temperatures of the canopy (foliage and soil) as well as soil moisture were also measured in order to study the effects of temperature and soil moisture on leaf photosynthesis. Sometimes, canopy reflectance, leaf reflectance and transmittance, and FPAR were also measured together with the items mentioned above in order to study the C3/C4 feature of different plants.

3.3.4. LST and Emissivity

[65] The observations of LST and emissivity on the ground were used to validate the LST retrieved from simultaneous airborne and satellite-borne thermography, which were mainly carried out in the FEAs in YK, HZZ and LZG, and occasionally in LZS and AR. Two thermal imagers, seven autorecording thermal infrared detectors, and fifteen handheld thermal radiometers were used for the LST observations.

Table 2. Airborne Remote Sensing Instruments Used in WATER

Remote Sensing Instrument	Major Characteristics of the Instrument[a]	Resolution (Flight Height of 1500 m)	Observation Items	Producer
L-band nonimaging microwave radiometer	Frequency: 1.413 GHz. bandwidth: 25 MHz. beam width: 15°. incident angle: 35°. polarization: V and H.	120~600 m[b]	Soil moisture, soil freeze/thaw status, and snow moisture	NEIGAE/CAS[c]
K-band nonimaging microwave radiometer	Frequency: 18.7 GHz. bandwidth: 400 MHz. incident angle: 0° (nadir looking). beam width: 12°. polarization: V.	100~400 m[b]	Soil moisture, soil freeze/thaw status, snow depth, and snow moisture	NEIGAE/CAS
Ka-band microwave imaging radiometer	Frequency: 36.0 GHz. bandwidth: 400 MHz. incident angle: 0°. beam width: 1.5°. polarization: V.	39 m	Snow depth	NEIGAE/CAS
Lidar system: LiteMapper 5600	Lidar: measurement range: 100 KHz. accuracy: 0.02 m. flight height: 200–1500 m above ground. laser beam divergence: ≤ 0.5 mrad. scan angle range: ± 22.5°. CCD: model: DigiCAM-H/22. focal length: 50 mm. 5440 × 4080 pixels, 50° total field of view.	Point cloud density: > 3 point m^{-2}, 0.1–0.2 m[d]	Canopy structure, NPP, DEM, forest height, land cover type, and tree crown size	IGI, Germany
VNIR push broom imaging spectrometer: PHI-II	400–850 nm, 124 bands, spectral resolution ≤ 5 nm, 0.7 mrad cross-track IFOV, 1.2 mrad along-track IFOV, 24° total field of view.	1.05 m	Biogeophysical parameters, biogeochemical parameters, vegetation classification, reflectance, and albedo	SITP/CAS
Shortwave infrared push broom imaging spectrometer: SWPHI	1000–2500 nm, 256 bands, spectral resolution ≤ 10 nm, 1.3 mrad cross-track IFOV, 1.0 mrad along-track IFOV, 24° total field of view.	1.95 m	Snow grain size, reflectance, albedo, and vegetation water content	SITP/CAS
Imaging spectrometer: OMIS-II	60 bands at 0.46–1.1 μm, 1 band at 1.55–1.75 μm, 2.08–2.35 μm, 3.0–5.0 μm, and 8.0–12.5 μm, 3 mrad IFOV, 73° total field of view.	4.5 m	Biogeophysical parameters, biogeochemical parameters, vegetation classification, reflectance, albedo, and LST	SITP/CAS
Wide-Angle Infrared Dual-mode Line/Area Array Scanner (WiDAS)	WiDAS is composed of two thermal imagers and four CCD cameras. Thermal imager: two bands (3.5–5 and 8–12 μm), 80° total field of view, seven observation angles: +40°, +30°, +20°, 0°, −20°, −30°, −40° (+forward, -backward). CCD camera: four bands (550, 650, 700, and 750 nm), 1392 × 1040 pixels, 60° total field of view, five observation angles: +29°, +20°, 0°, −20°, −29°.	7.86 m for thermal imager, 1.2 m for CCD camera	LST, canopy temperature, snow surface temperature, emissivity, soil moisture, biogeophysical parameters, biogeochemical parameters, reflectance, and albedo	IRSA/CAS and BNU

[a]V, vertical; H, horizontal.
[b]The higher resolution is in correspondence with a flight height of 350 m.
[c]Abbreviations for the institutions are listed in the Notation section.
[d]When flight height is about 800 m.

3.3.5. Reflectance and Albedo

[66] The spectral reflectance of various vegetations, for example, maize, wheat, clover, and desert vegetation were measured with wavelengths from 350 to 2500 nm using the ASD spectrometer. The leaf reflectance and transmittance were measured using a LI-1800-12S external integrating sphere (390–1100 nm) or a ASD leaf clip (350–2500 nm).

[67] BRDF was measured using a newly designed goniometer, which can view the canopy in the upper hemisphere at a maximum height of 5 m. For row-structured crops like maize and wheat, BRDF was measured in four important planes, which were the solar principle and cross-principle planes, along and cross row planes. For other natural targets which showed homogeneous or random distribution, for example, alfalfa and reed, BRDF were generally measured only in the principle and cross-principle planes. The viewing zenith angles were from −60° to 60° with an interval of 5° and 10° in LZS and YK, respectively.

[68] In addition to the spectral reflectance and BRDF, albedo was acquired by comparing upwelling to downwelling solar radiation measured using six portable Kipp & Zonen CM 22 pyranometers. Meanwhile, the albedos of typical ground cover were continuously measured at several AMSs (see section 3.4).

3.4. Hydrometeorology Experiment

[69] In coordination with the cold region, arid region, and forest hydrology experiments, the aim of the hydrometeorology experiment was to establish and maintain a AMS and flux tower network, collect data from existing observation network including operational meteorological and hydrological stations, carry out atmospheric sounding measurements, and conduct a Doppler radar precipitation observation.

3.4.1. Network of AMS and Flux Tower

[70] A network of hydrometeorological and flux observations was established in the upper and middle reaches of the Heihe River Basin. The network was composed of 7 newly installed AMSs, 4 new EC systems, 2 new LAS, 5 existing AMSs, 2 existing ECs, 8 Chinese Meteorological Administration (CMA) operational meteorological stations, and 34 CMA regional meteorological stations. They are distributed in three KEAs of WATER, covering an area of
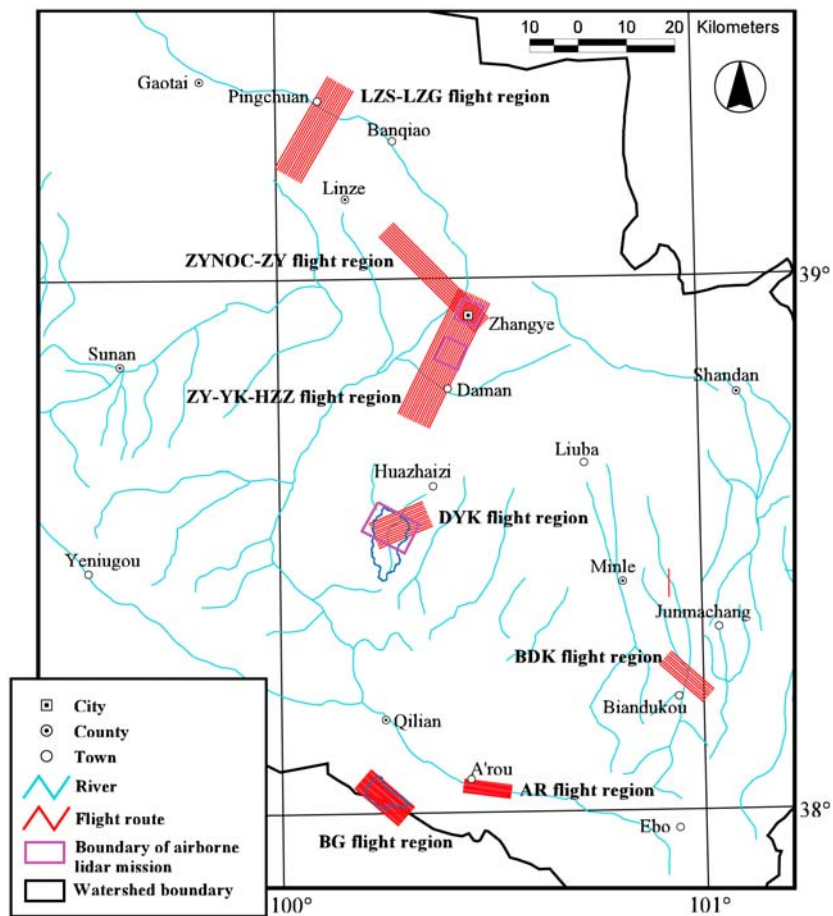
Figure 8. Flight regions of the airborne missions in WATER.

23,700 km^2 (Figure 6). The AMS and flux tower network was composed of conventional stations, key stations, and superstations.

[71] 1. The conventional stations were to observe the following surface meteorological variables: surface wind direction, wind speed, air temperature, air humidity, and air pressure; precipitation and pan evaporation; LST, soil tem-

perature profile, and soil moisture profile; sky condition (cloud cover, visibility, sand dust, etc.) and synoptic process; and frost depth by frost tube.

[72] 2. The key stations observed the following items: all of the observation items of conventional stations; multilayer gradient observation of wind speed, air temperature, and air humidity; total solar radiation, reflective shortwave radia-

Table 3. Flight Regions of the Airborne Remote Sensing Missions in WATER[a]

Name	Experiment	Size (km)	Observation Items	Onboard Instruments
LZS-LZG flight region	Arid region hydrology	13 × 22	LST, canopy temperature, soil moisture, ET, reflectance, albedo, and biogeophysical parameters	OMIS-II, WiDAS, and microwave radiometer
ZYNOC-ZY flight region	Arid region hydrology	9 × 28	LST, reflectance, and albedo	WiDAS
ZY-YK-HZZ flight region	Arid region hydrology	15 × 29	LST, canopy temperature, soil moisture, ET, reflectance, albedo, biogeophysical parameters, biogeochemical parameters, and structure parameters of crop	OMIS-II, WiDAS, lidar, CCD, and microwave radiometer
DYK flight region	Forest hydrology	13 × 12	Structure parameters of forest, NPP, DEM, LST, canopy temperature, reflectance, albedo, and biogeophysical parameters	Lidar, CCD, OMIS-II, and WiDAS
BG flight region	Cold region hydrology	18 × 12	Snow depth, snow moisture, snow grain size, reflectance, and albedo	Microwave radiometer, PHI-II, and SWPHI
AR flight region	Cold region hydrology	10 × 10	Soil freeze/thaw status, soil moisture, LST, ET, reflectance, and albedo	Microwave radiometer and WiDAS
BDK flight region	Cold region hydrology	8 × 12	Soil freeze/thaw status, soil moisture, reflectance, and albedo	Microwave radiometer and WiDAS

[a]Abbreviations are listed in the Notation section.

Table 4. Summary of the Airborne Missions in WATER[a]

Date	Time (BJT)	Airborne Remote Sensing Instrument	FEA	Satellite Data Acquired	Ground-Based Observations	Aims	Weather
19 Mar	0920–1250	L and K bands microwave radiometer	AR and BDK	PRISM	Soil moisture, LST, roughness, and GPR in AR	Soil freeze/thaw status and soil moisture	Partly cloudy
21 Mar	0803–1136	L and K bands microwave radiometer	BDK	ASAR	Soil moisture and LST	Soil freeze/thaw status and soil moisture	Sunny
22 Mar	1045–1415	PHI-II and SWPHI	BG	Hyperion	Depth, density, grain size, spectral reflectance, albedo, emissivity, and surface temperature of snow; optical properties of atmosphere; and GPR	Snow cover extent, snow grain size, reflectance, and albedo	Sunny
24 Mar	0858–1419	PHI-II and SWPHI	BG	NA	Depth, density, grain size, spectral reflectance, albedo, emissivity, surface temperature, and evaporation of snow; optical properties of atmosphere; and ground-based microwave radiometer	Snow cover extent, snow grain size, reflectance, and albedo	Sunny
25 Mar	1310–1730	PHI-II and SWPHI	YK, HZZ, ZYNOC and ZY	ASTER	None	Reflectance and albedo	Partly cloudy
29 Mar	0848–1256	Ka and K bands microwave radiometer	BG	NA	Depth, evaporation, grain size, density, and surface temperature of snow; and optical properties of atmosphere	Snow depth	Sunny
30 Mar	1241–1539	Ka and K bands microwave radiometer	BG	NA	Depth, evaporation, grain size, density, and surface temperature of snow	Snow depth	Sunny
1 Apr	0806–1115	L and K bands microwave radiometer	AR	ASTER	Soil moisture, LST; optical properties of atmosphere	Soil freeze/thaw status	Sunny
1 Apr	1247–1636	L-band microwave radiometer and thermal imager	AR and BG	ASTER	Soil moisture and LST in AR; snow depth and evaporation in BG	Soil freeze/thaw status, LST	Sunny
25 May	0948–1459	L and K bands microwave radiometer	LZG, LZS, and BDK	NA	Soil moisture, LST, roughness, ground-based microwave radiometer, and GPR in BDK	Soil moisture	Cloudy
30 May	1117–1555	WiDAS	LZS, LZG, ZY, YK, and HZZ	Hyperion, AASTR, and MERIS	LST, soil moisture, spectral reflectance, albedo, ET, LAI, vegetation coverage, vegetation structure, photosynthesis, and optical properties of atmosphere	LST, canopy temperature, biogeophysical parameters, and biogeochemical parameters	Sunny
31 May	1057–1404	WiDAS	DYK, AR, and BDK	NA	LST, soil moisture, reflectance, emissivity; GPR in AR	LST, canopy temperature, biogeophysical parameters	Partly cloudy
1 Jun	1317–1614	WiDAS	ZY and YK	NA	LST, spectral reflectance, albedo, emissivity, vegetation structure, and optical properties of atmosphere in YK	LST, canopy temperature, and biogeophysical parameters	Partly cloudy
4 Jun	0950–1530	OMIS-II	ZY, YK, HZZ, and DYK	Hyperion	Spectral reflectance, LST, LAI, structure parameter of forest, ground-based lidar, and optical properties of atmosphere in HZZ	Reflectance, biogeophysical parameters, biogeochemical parameters	Sunny in ZY, YK, and HZZ; partly cloudy in DYK
6 Jun	0928–1312	OMIS-II	LZS and LZG	MISR and MERIS	Spectral reflectance, LST, ET, photosynthetically active radiation (PAR), LAI, optical properties of atmosphere, and optical properties of atmosphere in LZG	Reflectance, ET, and biogeophysical parameters	Sunny
15 Jun	1200–1531	OMIS-II	LZS and LZG	AATSR and MERIS	Spectral reflectance, LST, ET, PAR, and optical properties of atmosphere in LZG	Reflectance, ET, and biogeophysical parameters	Sunny
16 Jun	1430–1811	OMIS-II	ZY, YK, and HZZ	NA	LST, photosynthesis, and vegetation structure	Reflectance, biogeophysical parameters, and biogeochemical parameters	Partly cloudy
20 Jun	1000–1551	Lidar	DYK, ZY, YK, and HZZ	MISR	LAI, PAR, soil moisture, soil temperature, structure parameters of forest, and chlorophyll	Canopy structure and DEM	Cloudy
23 Jun	1037–1545	Lidar, CCD, and thermal imager	DYK	NA	Structure parameters of forest	Canopy structure and DEM	Sunny
24 Jun	1020–1427	lidar and CCD	DYK	MERIS	Structure parameters of forest	Canopy structure and DEM	Sunny

Table 4. (continued)

Date	Time (BJT)	Airborne Remote Sensing Instrument	FEA	Satellite Data Acquired	Ground-Based Observations	Aims	Weather
29 Jun	1040–1521	WiDAS	ZY, YK, HZZ, LZS, LZG, and ZYNOC	MISR	LST, canopy temperature, spectral reflectance, albedo, FPAR, LAI, soil moisture, thermal infrared spectrum, photosynthesis, chlorophyll, biogeochemical parameters, structure parameters of maize; optical properties of atmosphere in YK; and BRDF in LZS	LST, canopy temperature, reflectance, biogeophysical parameters, and biogeochemical parameters	Partly cloudy
4 Jul	0948–1414	L and K bands microwave radiometer	BDK, LZS, and LZG	SPOT5, AATSR, and MERIS	Soil moisture and surface temperature	Soil moisture	Partly cloudy
7 Jul	1043–1533	WiDAS	ZY, YK, HZZ, AR, and BDK	TM, AATSR, and MERIS	LST, spectral reflectance, albedo, FPAR, soil moisture, photosynthesis, chlorophyll, and optical properties of atmosphere in YK	LST, canopy temperature, and biogeophysical parameters	Sunny in ZY and BDK; cloudy in AR
8 Jul	1000–1340	L and K bands microwave radiometer	LZS and LZG	ASAR	Soil moisture, LST, and ground-based C-band scatterometer	Soil moisture	Partly cloudy
11 Jul	1126–1430	WiDAS	LZS, LZG, ZYNOC, ZY, and YK	MERIS	LST, spectral reflectance, albedo, ET, FPAR, vegetation coverage, photosynthesis, optical properties of atmosphere in LZG; ground-based C-band scatterometer	LST, canopy temperature, and biogeophysical parameters	Sunny

aAbbreviations are listed in the Notation section. BJT denotes Beijing time.

tion, land surface longwave radiation, and atmospheric longwave radiation; soil temperature and soil moisture profile at deeper soil layers and soil heat flux at shallow layer; and LST by thermal infrared radiometer.

[73] 3. The superstations observed the following items: all of the observation items of key stations; sensitive heat flux, latent heat flux, and CO_2 flux (optional); and other selective observation items such as forest hydrology.

[74] All of the CMA operational and regional stations were defined as conventional stations in WATER. The data from the conventional stations were collected in cooperation with CMA local offices. Other stations were identified as key stations and superstations. Their details are listed in Table 1.

3.4.2. Precipitation

[75] The precipitation shows a strong spatial heterogeneity in mountain cryosphere as well as in arid region, so it is a critical task to improve the accuracy of the measurement of precipitation in WATER. The 714XDP X-band dual-linear polarization Doppler weather radar mounted on a truck, with a horizontal resolution of 150 m, was employed during the IOP of WATER to obtain high-resolution observations of precipitation. It was placed at AR (100.45°E, 38.06°N, 3001 m) during the cold region hydrology experiment, where it was capable of covering the whole Babao River Basin. In the forest and arid region hydrology experiments, it was moved to Liuba (100.66°E, 38.73°N, 1668 m) in Minle county, where it covered the Dayekou watershed and the whole arid region hydrology experimental area in cooperation with the CMA operational Doppler radar in Zhangye (Figures 6 and 7).

[76] Two precipitation particle drop size analyzers and a number of rain gauges, including 33 simple rain gauges, 29 RG3-M rain gauges, and a rain gauge network along the mountain slope with a height difference of every 200~300 m were installed during the IOP in the cold region, arid region and forest hydrology experimental areas, respectively. All these newly installed rain gauges, along with the AMSs and operational hydrological stations in the Heihe River Basin, provided a precipitation measurement network for WATER (Figure 7), making it possible to produce a high-resolution precipitation data set.

3.4.3. Runoff and Other Hydrological Variables

[77] The runoff observations in WATER were operated by the local hydrological stations. In addition, two new runoff gauges were built in Binggou and Dayekou watersheds, which were FEAs of cold region and forest hydrology experiments, respectively. The irrigation data were collected with the cooperation of local water management bureau. Groundwater levels were monitored on a daily basis using 36 existing wells in middle reaches of the Heihe River Basin (Figure 7).

3.4.4. Atmospheric Sounding and Aerosol Observation

[78] Atmospheric correction is a precondition for quantitative remote sensing, therefore, the observation of optical properties of atmosphere is very important. During the IOP, the air temperature and humidity profiles and aerosol properties were measured concurrently with airborne missions and satellite overpasses.

[79] The atmospheric sounding was carried out using the digital sounder RS92 produced by VAISALA, which can measure the profiles of air temperature, air humidity, air

Table 5. Satellite Data Acquired in WATER[a]

Type	Remote Sensors	Observation Aims	Scale	Time
Very high resolution multi-spectral (1–5 m)	IKONOS, ALOS PRISM, Proba HRC, QuickBird, and SPOT5 HRG	Vegetation classification and mapping of the experimental area	FEA	Experiment planning period, IOP
High-resolution multispectral (10–120 m)	ASTER, ALOS AVNIR-2, CBERS-02B CCD, and TM	Reflectance, albedo, LST, snow surface temperature, snow cover extent, and biogeophysical parameters	KEA	IOP
Medium-resolution multispectral	CBERS-02B WFI, MERIS, and MODIS	Reflectance, albedo, LST, snow cover extent, and biogeophysical parameters	Whole Heihe River Basin	IOP, persistent observation period
Multiangle	MISR	biogeophysical parameters and BRDF	Whole Heihe River Basin	IOP
Imaging spectroscopy	Proba CHRIS and Hyperion	biogeophysical parameters, biogeochemical parameters, and snow grain size	FEA	POP and IOP
Thermal	AATSR	LST	KEA	IOP
SAR	Envisat ASAR, ALOS PALSAR, RADARSAT-2, and TerraSAR-X	Snow depth, soil freeze/thaw status, soil moisture, and structure parameters of forest	KEA and the whole Heihe River Basin	POP and IOP
Passive microwave remote sensing	AMSR-E	Soil freeze/thaw status, soil moisture, and snow depth	Whole Heihe River Basin	IOP, persistent observation period
Lidar	ICESat GLASS	Structure parameters of forest	Forest hydrology experimental area	IOP

[a]Abbreviations are listed in the Notation section.

pressure, latitudinal and longitudinal wind speeds, and altitude below 20,000 m in the troposphere, with a frequency of 2 s. In total, 20 atmospheric soundings using GPS-tracking balloons were carried out during the IOP in different FEAs. Most of them were concurrent with airborne missions of VNIR, thermal infrared, and hyperspectral instruments, and some during the overpass of high-resolution satellite remote sensing, particularly Hyperion and CHRIS.

[80] The optical properties of atmosphere, particularly those of aerosol were measured using CE318 Sun photometers, which were installed in BG in the cold region hydrology experiment, and in YK, ZY and LZG in the arid region hydrology experiment. The total optical depth, aerosol optical depth, Rayleigh scattering coefficient, ozone in ultraviolet to near infrared wavelength, column water vapor in 936 nm, particle size spectrum and phase function were then retrieved from these observations.

4. Airborne Missions

4.1. Aircraft and Airborne Remote Sensing Instruments

[81] The Y-12 (airplane ID: B-3820), which is a fixed-wing aircraft with a ceiling altitude of 6000 m, was operated in WATER for the airborne missions. The aircraft was based on Zhangye airport, within a half-hour flight of each experimental area. A range of airborne remote sensing instruments were employed in WATER, including passive microwave radiometer, imaging spectrometer, thermal imager, lidar, and CCD camera (Table 2).

4.2. Airborne Missions

[82] Seven flight regions were identified as being required, with three in the cold region, one in the forest region, and another three in the arid region hydrology experimental areas. The flight routes were designed taking into consideration of full coverage of all FEAs, effectiveness, safety, and the resolution of airborne remote sensing instruments. Figure 8 shows the flight routes of the airborne missions in WATER. The corresponding observation items and onboard instruments are listed in Table 3.

[83] In total, 25 missions were flown, with 8 in the cold region, 4 in the forest region, and 13 for arid region hydrology experiment. The flying time amounted to 110 h. Most of the airborne missions were designed to fly during the overpass of satellite sensors for concurrent analysis. Details are summarized in Table 4.

5. Satellite Data Acquisition

[84] Satellite remote sensing was a very important part of WATER. Various satellite remote sensing data from VNIR, thermal infrared, active microwave, passive microwave, and lidar sensors were collected by data sharing programs, international cooperation and a limited commercial purchase. Since many new satellites were launched in recent years, the satellite data acquired by WATER were more diverse than in previous land surface experiments. The high-resolution satellite data acquired during the POP and IOP were estimated to be above 200 scenes, and the medium and coarse resolution remote sensing data were obtained on a daily basis. The satellite data acquired in WATER are listed in Table 5.

6. Summary and Prospect

[85] WATER, aimed to improve the observability, understanding, and predictability of hydrological and related ecological processes at a catchmental scale, was carried out in the second largest inland river basin of arid region in northwest China, the Heihe River Basin. As an interdisciplinary, intensive, coordinated and multiscale experiment, the data obtained from the field campaigns in WATER, both acquired from airborne and satellite-borne remote sensing, and observed on the ground, were going to be used to generate a high-resolution and spatiotemporally consistent data set for the development of integrated watershed models.

[86] The airborne-mission leading field campaigns have been completed. The data acquisition can be concluded as a great success, with numerous amounts of data, most of them concurrent in time and cross-scale in space, being acquired

as planned. The data set, including raw data, calibrated data and data products in different levels, after quality control, will be available to the experiment participants for analysis, and later to the science community and the public through the WIS.

[87] The watershed science will have a more comprehensive data set to rely on. The integrated watershed models and various algorithms to retrieve hydrological and ecological variables from remote sensing can be tested, validated, improved and later be integrated into the catchment-scale land/hydrological data assimilation system, which should be capable of generating high-resolution and spatiotemporal consistent data sets and thus improve the predictability of water cycle in a river basin.

[88] Potentially, WATER will also have some practical consequences. The improved understanding of water cycle at a catchment scale, particularly for the inland river basins in arid region, is valuable for water management. The multisource remote sensing data can be used to develop spatially explicit decision supporting tools. Therefore, the integrated river basin management could benefit from WATER.

[89] WATER will now move on to the rewarding part, that is, the analysis of data, and the validation, modification, and development of various models. Revisits to the field are also anticipated when necessary. Challenges will also come in the next step, but we are confident to see the accomplishment of WATER within the next few years.

[90] A more comprehensive catchment-scale experiment is under discussion, and the NSFC is going to initialize its watershed science plan [*Cheng et al.*, 2008b]. It is confident to see a booming of watershed science study, led by more well-designed and sophisticated experiments. WATER, hopefully, will serve as a model for future practice.

Notation

AATSR	Advanced Along-Track Scanning Radiometer.
ALI	Advanced Land Imager.
ALOS	Advanced Land Observing Satellite.
AMS	Automatic Meteorological Station.
AMSR-E	Advanced Microwave Scanning Radiometer–Earth Observing System.
ASAR	Advanced Synthetic Aperture Radar.
ASD	Analytical Spectral Device.
ASTER	Advanced Spaceborne Thermal Emission and Reflection Radiometer.
AVNIR-2	Advanced Visible and Near Infrared Radiometer–2.
BRDF	bidirectional reflectance distribution function.
CAS	Chinese Academy of Sciences.
CBERS-02B CCD	China-Brazil Earth Resources Satellite-02B CCD.
CBERS-02B WFI	China-Brazil Earth Resources Satellite-02B Wide Field Imager.
CCD	charge-coupled device.
CERN	Chinese Ecosystem Research Network.
CHRIS	Compact High-Resolution Imaging Spectrometer.
CLPX	Cold Land Processes Field Experiment.
CMA	Chinese Meteorological Administration.
DEM	digital elevation model.
EC	Eddy Covariance.
Envisat	Environmental Satellite.
ESA	European Space Agency.
ET	evapotranspiration.
FPAR	Fraction of Photosynthetically Active Radiation.
FOV	field of view.
GCM	general circulation model.
GLAS	Geoscience Laser Altimeter System.
GPR	Ground Penetrating Radar.
GPS	Global Positioning System.
HAPEX	Hydrological and Atmospheric Pilot Experiment in the Sahel.
HEIFE	Heihe River Basin Field Experiment.
Hyperion	Earth Observing 1 (EO-1) hyperspectral imaging instrument.
ICESat	Ice, Cloud and Land Elevation Satellite.
IFOV	instantaneous field of view.
IKONOS	A very high resolution commercial Earth observation satellite.
IMGRASS	Inner Mongolia Semiarid Grassland Soil-Vegetation-Atmosphere Interaction.
JAXA	Japan Aerospace Exploration Agency.
LAD	leaf angle distribution.
LAI	leaf area index.
LAS	Large Aperture Scintillometer.
lidar	Light Detection and Ranging.
LST	Land Surface Temperature.
MERIS	Medium Resolution Imaging Spectrometer.
MISR	Multiangle Imaging Spectroradiometer.
MODIS	Moderate Resolution Imaging Spectroradiometer.
MOST	Ministry of Science and Technology of China.
NPP	Net Primary Production.
NSFC	National Natural Science Foundation of China.
NWC-ALIEX	Field Experiment on Air-Land Interaction in the Arid Area of Northwest China.
PALSAR	Phased Array Type L-band Synthetic Aperture Radar.
PAR	photosynthetically active radiation.
PRISM	Panchromatic Remote-Sensing Instrument for Stereo Mapping.
PROBA	Project for On-Board Autonomy.
PROBA HRC	PROBA High-Resolution Camera.
QuickBird	a very high resolution commercial Earth observation satellite.
RADARSAT-2	a Canada Earth observation satellite with multiple polarization modes SAR boarded.
SAR	synthetic aperture radar.
SMTMS	Soil Moisture and Temperature Measurement System.

SPOT5 HRG SPOT5 High-Resolution Geometry.
TDR time domain reflectometer.
TerraSAR-X a German Radar satellite with X-band SAR.
TM thematic mapper.
VNIR visible and near infrared.

Abbreviations used specifically in the paper
AR A'rou.
BDK Biandukou.
BG Binggou watershed.
DYK Dayekou watershed.
ES experiment site.
ESP elementary sampling plot.
FEA foci experimental area.
HZZ Huazhaizi.
IOP intensive observation period.
KEA key experimental area.
LZG Linze grassland.
LZS Linze station.
PLG Pailugou watershed.
POP pre-observation period.
WATER Watershed Allied Telemetry Experimental Research.
WiDAS Wide-Angle Infrared Dual-mode Line/Area Array Scanner.
WIS WATER information system.
YK Yingke oasis.
ZY Zhangye city.
ZYNOC national observatory on climatology at Zhangye.

Leading institutions for WATER
CAREERI Cold and Arid Regions Environmental and Engineering Research Institute, CAS.
IRSA Institute of Remote Sensing Applications, CAS.
BNU Beijing Normal University.
IFRIT Institute of Forest Resource Information Techniques, Chinese Academy of Forestry.

Participating institutions for WATER
UESTC University of Electronic Science and Technology of China.
SITP Shanghai Institute of Technical Physics, CAS.
IGSNRR Institute of Geographic Sciences and Natural Resources Research, CAS.
AWRCFQM Academy of Water Resources Conservation Forest in Qilian Mountains, Gansu Province.
PKU Peking University.
NJU Nanjing University.
EGI Xinjiang Institute of Ecology and Geography, CAS.
NEIGAE Northeast Institute of Geography and Agroecology, CAS.
GUCAS Graduate University of Chinese Academy of Sciences.

IAM Institute of Arid Meteorology, CMA, Lanzhou.
IDM Institute of Desert Meteorology, CMA, Urumqi.
CSSAR Center for Space Science and Applied Research, CAS.
CEODE Center for Earth Observation and Digital Earth, CAS.
UH University of Heidelberg, Germany.
WHU Wuhan University.
LZU Lanzhou University.
CAAS Chinese Academy of Agricultural Sciences.
NERCITA National Engineering Research Center for Information Technology in Agriculture.
SNU Sichuan Normal University.
CNU Capital Normal University.
SCAU South China Agricultural University.

Supporting institutions for WATER
CFGAC Zhong Fei General Aviation Company.
CFTE Chinese Flight Test Establishment.
G-ENERGY Guangxi G-Energy Information Engineering Company, Ltd.
BTSC Beijing Techno Solution Company, Ltd.

References

Arnold, J. G., and N. Fohrer (2005), SWAT2000: Current capabilities and research opportunities in applied watershed modeling, *Hydrol. Processes*, *19*(3), 563–572, doi:10.1002/hyp.5611.

Avissar, R., and C. A. Nobre (2002), Preface to special issue on the Large-Scale Biosphere-Atmosphere Experiment in Amazonia (LBA), *J. Geophys. Res.*, *107*(D20), 8034, doi:10.1029/2002JD002507.

Cheng, G. D., et al. (2008a), Integrated model development and modeling environment building for interdisciplinary studies in the Heihe River Basin (in Chinese), report, 352 pp., Cold and Arid Reg. Environ. and Eng. Res. Inst., Chin. Acad. of Sci., Lanzhou, China.

Cheng, G. D., H. L. Xiao, C. Z. Li, J. Ren, and S. Wang (2008b), Water saving eco-agriculture and integrated water resources management in the Heihe River Basin, northwest China (in Chinese), *Adv. Earth Sci.*, *23*(7), 661–665.

Cline, D., R. E. Davis, W. Edelstein, J. Hilland, K. McDonald, S. Running, J. Way, and J. van Zyl (1999), Cold Land Processed Field Experiment

plan, report, Cold Land Proc. Working Group, NASA Earth Sci. Enterprise Land Surf. Hydrol. Program, Greenbelt, Md.

Dai, Y., et al. (2003), The common land model, *Bull. Am. Meteorol. Soc.*, *84*(8), 1013–1023, doi:10.1175/BAMS-84-8-1013.

Goovaerts, P. (1997), *Geostatistics for Natural Resource Evaluation*, 483 pp., Oxford Univ. Press, New York.

Goutorbe, J. P., et al. (1994), HAPEX-SAHEL: A large-scale study of land-atmosphere interactions in the semiarid tropics, *Ann. Geophys.*, *12*(1), 53–64, doi:10.1007/s00585-994-0053-0.

Hu, Y. Q., Y. X. Gao, J. M. Wang, G. L. Ji, Z. B. Shen, L. S. Cheng, J. Y. Chen, and S. Q. Li (1994), Some achievements in scientific research during HEIFE (in Chinese), *Plateau Meteorol.*, *13*(3), 225–236.

Huang, T. Q., et al. (2007), Project arrangement and primal progress in the second phase of the CAS Action Plan for West Development (in Chinese), *Adv. Earth Sci.*, *22*(9), 888–895.

Hufkens, K., J. Bogaert, Q. H. Dong, L. Lu, C. L. Huang, M. G. Ma, T. Che, X. Li, F. Veroustraete, and R. Ceulemans (2008), Impacts and uncertainties of upscaling of remote-sensing data validation for a semi-arid woodland, *J. Arid Environ.*, *72*(8), 1490–1505, doi:10.1016/j.jaridenv.2008.02.012.

Justice, C., A. Belward, J. Morisette, P. Lewis, J. Privette, and F. Baret (2000), Developments in the 'validation' of satellite sensor products for the study of the land surface, *Int. J. Remote Sens.*, *21*(17), 3383–3390, doi:10.1080/014311600750020000.

Kang, E. S., G. D. Cheng, and Z. C. Dong (Eds.) (2002), *Glacier-Snow Water Resources and Mountain Runoff in the Arid Area of Northwest China (in Chinese)*, 304 pp., Sci. Press, Beijing.

Li, X., and G. D. Cheng (2008), On the watershed observing and modeling systems (in Chinese), *Adv. Earth Sci.*, *23*(7), 756–764.

Li, X., L. Lu, G.-D. Cheng, and H.-L. Xiao (2001), Quantifying landscape structure of the Heihe River Basin, northwest China using FRAGSTATS, *J. Arid Environ.*, *48*(4), 521–535, doi:10.1006/jare.2000.0715.

Li, X., et al. (2007), Watershed Airborne Telemetry Experimental Research (WATER) implementation plan (in Chinese), report, 122 pp., Cold and Arid Reg. Environ. and Eng. Res. Inst., Chin. Acad. of Sci., Lanzhou, China.

Li, X., et al. (2008), Simultaneous remote sensing and ground-based experiment in the Heihe River Basin: Scientific objectives and experiment design (in Chinese), *Adv. Earth Sci.*, *23*(9), 897–914.

Liang, S., H. Fang, M. Chen, C. J. Shuey, C. Walthall, C. Daughtry, J. Morisette, C. Schaaf, and A. Strahler (2002), Validating MODIS land surface reflectance and albedo products: Methods and preliminary results, *Remote Sens. Environ.*, *83*(1–2), 149–162, doi:10.1016/S0034-4257(02)00092-5.

Liang, X., D. P. Lettenmaier, E. F. Wood, and S. J. Burges (1994), A simple hydrologically based model of land-surface water and energy fluxes for general-circulation models, *J. Geophys. Res.*, *99*(D7), 14,415–14,428, doi:10.1029/94JD00483.

Lü, D. R., Z. Z. Chen, J. Y. Chen, G. C. Wang, J. J. Ji, H. B. Chen, and Z. L. Liu (2005), Study on soil-vegetation-atmosphere interaction in Inner-Mongolia semi-arid grassland (in Chinese), *Acta Meteorol. Sin.*, *63*(5), 571–593.

Sellers, P. J., F. G. Hall, G. Asrar, D. E. Strebel, and R. E. Murphy (1992), An overview of the First International Satellite Land Surface Climatology Project (ISLSCP) Field Experiment (FIFE), *J. Geophys. Res.*, *97*(D17), 18,345–18,371.

Sellers, P., et al. (1995), The Boreal Ecosystem–Atmosphere Study (BOREAS): An overview and early results from the 1994 field year, *Bull. Am. Meteorol. Soc.*, *76*(9), 1549–1577, doi:10.1175/1520-0477(1995)076<1549:TBESAO>2.0.CO;2.

Sellers, P. J., D. A. Randall, G. J. Collatz, J. A. Berry, C. B. Field, D. A. Dazlich, C. Zhang, G. D. Collelo, and L. Bounoua (1996), A revised land surface parameterization (SiB2) for atmospheric GCMs. Part I: Model formulation, *J. Clim.*, *9*(4), 676–705, doi:10.1175/1520-0442(1996)009<0676:ARLSPF>2.0.CO;2.

Sitch, S., et al. (2003), Evaluation of ecosystem dynamics, plant geography and terrestrial carbon cycling in the LPJ dynamic global vegetation model, *Global Change Biol.*, *9*(2), 161–185, doi:10.1046/j.1365-2486.2003.00569.x.

Surridge, B., B. Harris, S. A. F. Ben, and B. Harris (2007), Science-driven integrated river basin management: A mirage?, *Interdisciplinary Sci. Rev.*, *32*(3), 298–312.

Tian, Y., et al. (2002), Multiscale analysis and validation of the MODIS LAI product: II. Sampling strategy, *Remote Sens. Environ.*, *83*(3), 431–441, doi:10.1016/S0034-4257(02)00058-5.

Uhlenbrook, S., and S. A. F. Uhlenbrook (2006), Catchment hydrology: A science in which all processes are preferential, *Hydrol. Processes*, *20*(16), 3581–3585, doi:10.1002/hyp.6564.

Wang, G. X., and G. D. Cheng (1999), Water resource development and its influence on the environment in arid areas of China: The case of the Hei River basin, *J. Arid Environ.*, *43*(2), 121–131, doi:10.1006/jare.1999.0563.

Wang, H., M. J. Chen, and D. Y. Qin (2003), *Rational Allocation and Bearing Capacity of Water Resources in Northwest China (in Chinese)*, Yellow River Water Conservancy Press, Zhengzhou, China.

Wang, J. M. (1999), Land surface process experiments and interaction study in China: From HEIFE to IMGRASS and GAME-Tibet/TIPEX (in Chinese), *Plateau Meteorol.*, *18*(3), 280–294.

Wheater, H. S., , S. Sorooshian, and K. D. Sharma (Eds.) (2008), *Hydrological Modelling for Arid and Semi-Arid Areas*, 206 pp., Cambridge Univ. Press, New York.

Wigmosta, M. S., L. W. Vail, and D. P. Lettenmaier (1994), A distributed hydrology-vegetation model for complex terrain, *Water Resour. Res.*, *30*(6), 1665–1679, doi:10.1029/94WR00436.

Zhang, Q., et al. (2005), NWC-ALIEX and its research advances (in Chinese), *Adv. Earth Sci.*, *20*(4), 427–441.

Zhang, R. H. (1996), *Experimental Remote Sensing Models and Its Field Foundation (in Chinese)*, 284 pp., Sci. Press, Beijing.

_____

T. Che, R. Chu, Z. Hu, R. Jin, X. Li, M. Ma, Y. Ran, P. Su, J. Wang, and W. Wang, Cold and Arid Regions Environmental and Engineering Research Institute, Chinese Academy of Sciences, 320 West Donggang Road, Gansu Province, Lanzhou 730000, China. (lixin@lzb.ac.cn)

E. Chen and Z. Li, Institute of Forest Resource Information Techniques, Chinese Academy of Forestry, Beijing 100091, China.

Y. Chen, School of Automation, University of Electronic Science and Technology of China, Chengdu 610054, China.

X. Li, Q. Liu, Q. Liu, Z. Niu, Q. Xiao, and X. Xin, Institute of Remote Sensing Applications, Chinese Academy of Sciences, Beijing 100101, China.

S. Liu, H. Ren, J. Wang, G. Yan, and L. Zhang, School of Geography and Remote Sensing Science, Beijing Normal University, Beijing 100875, China.